Alexandria Engineering Journal (2016) xxx, xxx–xxx

HOSTED BY

ELSEVIER

Alexandria University

Alexandria Engineering Journal

www.elsevier.com/locate/aej
www.sciencedirect.com

ORIGINAL ARTICLE

Particulate suspension slip flow induced by peristaltic waves in a rectangular duct: Effect of lateral walls

Safia Akram [a,*], **Kh.S. Mekheimer** [b,c], **Y. Abd Elmaboud** [d,e]

[a] *Department of Basic Sciences, MCS, National University of Sciences and Technology, Islamabad 4400, Pakistan*
[b] *Mathematics Department, Faculty of Science, Taif University Hawia, P.O. Box 888, Taif, Saudi Arabia*
[c] *Mathematics Department, Faculty of Science, Al-Azhar University, Nasr City, 11884 Cairo, Egypt*
[d] *Mathematics Department, Faculty of Science and Arts, Khulais, King Abdulaziz University (KAU), Saudi Arabia*
[e] *Mathematics Department, Faculty of Science, Al-Azhar University(Assiut Branch), Assiut, Egypt*

Received 29 March 2015; revised 19 September 2016; accepted 20 September 2016

KEYWORDS

Fluid suspension;
Lateral walls;
Peristaltic pumping;
Partial slip

Abstract This paper looks at the influence of lateral walls on peristaltic transport of a particle fluid suspension model applied in a non-uniform rectangular duct with slip boundaries. The peristaltic waves propagate on the horizontal sidewalls of a rectangular duct. The flow analysis has been developed for low Reynolds number and long wavelength approximation. Exact solutions have been established for the axial velocity and stream function. The effects of aspect the ratio β (ratio of height to width) and the volume fraction density of the particles C on the pumping characteristics are discussed in detail. The expressions for the pressure rise and friction forces on the wall of a rectangular duct were computed numerically and were plotted with variation of the flow rate for different values of the parameters. It is observed that in the peristaltic pumping ($\Delta p > 0, Q > 0$) and retrograde pumping ($\Delta p > 0, Q < 0$) regions the pumping rate increases with an increase in M, while in the copumping region ($\Delta p < 0, Q > 0$) the behavior is quite opposite. Furthermore it is also observed that the pressure rise increases in the upper half of the channel and decreases in the lower half of the channel with the increase in l_{slip} parameter.

1. Introduction

In the recent years peristaltic transport becomes an important subject for the researcher in biofluid. The peristaltic transport is very important because, it is a primary transport mechanism inherent in many tubular organs of the human body such as

* Corresponding author.
E-mail addresses: drsafiaakram@gmail.com, safia_akram@yahoo.com (S. Akram).
Peer review under responsibility of Faculty of Engineering, Alexandria University.

http://dx.doi.org/10.1016/j.aej.2016.09.011

the gastrointestinal tract, the urethra, the ureter and arterioles. The mechanism of peristaltic transport has been employed for industrial applications such as sanitary fluid transport, blood pumps in heart lung machine and transport of corrosive fluids. Peristaltic flow is generated in a channel (or a circular tube) when a progressive wave travels along the wall. Many studies have been carried out for understanding the characteristics of the transport mechanism associated with peristaltic flow under the assumption of low Reynolds number and infinitely long wavelength such as Jaffrin and Shapiro [1] explained the basic principles of peristaltic pumping and brought out clearly the significance of the various parameters governing the flow. A number of analytical, numerical and experimental recent studies of peristaltic flows of different fluids have been reported [2–13].

The theory of the two phase fluid is very useful in understanding a number of diverse physical problems including powder technology, fluidization. The continuum theory of mixtures is applicable to hydrodynamics of biological systems, because it provides an improved understanding of diverse subjects such as diffusion of proteins, the rheology of blood, swimming of micro-organisms and particle deposition. The model of a particulate suspension with peristaltic transport is investigated by many authors [14–18]. There are a recent few studies take into account the effect of the sidewalls in peristaltic transport such as Reddy et al. [19], and Nadeem and Akram [20]. None of the previous studies take into consideration slip boundaries and the sidewall effects especially in the non-uniform channel when the fluid model is a two phase fluid. So our motivation was to study the influence of lateral walls on peristaltic transport of a particle fluid suspension model applied in a non-uniform rectangular duct with slip boundaries.

2. Mathematical formulation

Let us consider the two-phase (fluid particles) flow in a non-uniform duct of rectangular cross section. The duct walls are flexible, and an infinite train of sinusoidal waves propagate with constant velocity c along the walls parallel to the XY plane in the axial direction. Cartesian coordinate system (X, Y, Z) is with X, Y, and Z axes corresponding to axial, lateral, and vertical directions, respectively, of a rectangular duct. We assume that there is no flow in the lateral direction. So, the velocity vector in this direction will be zero. The sinusoidal waves propagating along the channel walls are of the following forms:

$$Z' = H'(X', t') = \pm a \pm kx \pm b \sin\left[\frac{2\pi}{\lambda}(X' - ct')\right], \tag{1}$$

where a is the half width of the channel, b is amplitude of the wave, λ is the wavelength, d is the channel width, $k(\ll 1)$ is a constant whose magnitude depends on the length of the channel, c is the velocity of propagation, and t' is the time. The equations governing the conservation of mass and linear momentum for both the fluid and particle phases using a continuum approach are expressed as follows:

Fluid phase

$$\frac{\partial}{\partial X'}((1-C)U'_f) + \frac{\partial}{\partial Z'}((1-C)V'_f) = 0, \tag{2}$$

$$(1-C)\rho_f\left(\frac{\partial U'_f}{\partial t'} + U'_f\frac{\partial U'_f}{\partial X'} + V'_f\frac{\partial U'_f}{\partial Z'}\right) = -(1-C)\frac{\partial P'}{\partial X'} + (1-C)\mu_s(C)\nabla^2 U'_f + CS\left(U'_P - U'_f\right), \tag{3}$$

$$(1-C)\rho_f\left(\frac{\partial V'_f}{\partial t'} + U'_f\frac{\partial V'_f}{\partial X'} + V'_f\frac{\partial V'_f}{\partial Z'}\right) = -(1-C)\frac{\partial P'}{\partial Z'} + (1-C)\mu_s(C)\nabla^2 V'_f + CS\left(V'_P - V'_f\right), \tag{4}$$

Particulate phase

$$\frac{\partial}{\partial X'}(CU'_P) + \frac{\partial}{\partial Z'}(CV'_P) = 0, \tag{5}$$

$$C\rho_P\left(\frac{\partial U'_P}{\partial t'} + U'_P\frac{\partial U'_P}{\partial X'} + V'_P\frac{\partial U'_P}{\partial Z'}\right) = -C\frac{\partial P'}{\partial X'} + CS\left(U'_f - U'_P\right), \tag{6}$$

$$C\rho_P\left(\frac{\partial V'_P}{\partial t'} + U'_P\frac{\partial V'_P}{\partial X'} + V'_P\frac{\partial V'_P}{\partial Z'}\right) = -C\frac{\partial P'}{\partial Z'} + CS\left(V'_f - V'_P\right), \tag{7}$$

where $\left(U'_f,\ V'_f\right)$ and $\left(U'_P,\ V'_P\right)$ are the velocity components of the fluid and the particle phase respectively, P' is the pressure, C is the volume fraction density of the particles [17], $\mu_s(C)$ is the mixture viscosity (effective or apparent viscosity of suspension) and S is the drag coefficient of interaction for the force exerted by one phase on the other. The expression for the drag coefficient of interaction, S and the empirical relation for the velocity of the suspension, μ_s for the present problem is selected as done by Srivastava and Saxena [17]

$$S = \frac{9}{2}\frac{\mu_0}{a_0^2}\lambda'(C),$$

$$\lambda'(C) = \frac{4 + [8C - 3C^2]^{\frac{1}{2}} + 3C}{(2-3C)^2}, \tag{8}$$

$$\mu_s = \mu_s(C) = \frac{\mu_0}{1-mC},$$

$$m = 0.070\exp\left[2.49C + \frac{1107}{T}\exp(-1.69C)\right], \tag{9}$$

where a_0 is the radius of each solid particle suspended in the fluid, μ_0 is the constant fluid viscosity and T is measured in absolute temperature (K^0). The formula (9) has been tested by Charm and Kurland [21] by using a cone and a plate viscometer, and it has been proclaimed that it is reasonably accurate up to $C = 0.6$.

Let us define a wave frame (x', y', z') moving with the velocity c away from the fixed frame (X', Y', Z') by the transformation

$$x' = X' - ct', y' = Y', \quad z' = Z', \quad u'_{f,p} = U'_{f,p} - c,$$
$$v'_{f,p} = V'_{f,p}, \quad p'(x,z) = P'(X,Z,t). \tag{10}$$

where $u'_{f,p}$ and $v'_{f,p}$ are the velocity components of fluid and particle respectively, p' and P' are the pressures in wave and fixed

frame respectively. Consider the following non-dimensional variables:

$$x=\frac{x'}{\lambda},\ y=\frac{y'}{d},\ z=\frac{z'}{a},\ \delta=\frac{a}{\lambda},\ u_p=\frac{u'_p}{c},\ u_f=\frac{u'_f}{c},\ t=\frac{ct'}{\lambda},$$
$$h=\frac{H'}{a},\ p=\frac{a^2p'}{\mu c\lambda},$$

$$\beta=\frac{a}{d},\ \phi=\frac{b}{a},\ v_f=\frac{v'_f}{c\delta},\ v_p=\frac{v'_p}{c\delta},\ Re=\frac{ac\rho_f}{\mu_s(1-C)},$$
$$M=\frac{sa^2}{\mu_s(1-C)},$$

$$N=\frac{sa^2\rho_f}{\rho_p\mu_s(1-C)},\ \bar{\mu}=\frac{\mu_s}{\mu},\ \bar{\rho}=\frac{\rho_p}{\rho_f}. \tag{11}$$

where β is an aspect ratio (aspect ratio $\beta<1$ means that height is less compared to width, and $\beta=0$ corresponds to a two-dimensional channel. When $\beta=1$, the rectangular duct becomes a square duct and for $\beta>1$, the height is more compared to width.). Re is a suspension Reynolds number, (M,N) are the suspension parameters, δ is the wave number, and ϕ is the amplitude ratio. In moving frame, the nondimensional equations of motion for both the fluid and particle phase are

$$\frac{\partial}{\partial x}((1-C)u_f)+\delta\frac{\partial}{\partial z}((1-C)v_f)=0, \tag{12}$$

$$Re\delta\bar{\mu}(1-C)\left(u_f\frac{\partial u_f}{\partial x}+v_f\frac{\partial u_f}{\partial z}\right)$$
$$=-\frac{\partial p}{\partial x}+\bar{\mu}\left(\delta^2\frac{\partial^2u_f}{\partial x^2}+\beta^2\frac{\partial^2u_f}{\partial y^2}+\frac{\partial^2u_f}{\partial z^2}\right)+MC\bar{\mu}(u_p-u_f), \tag{13}$$

$$Re\delta^3\bar{\mu}(1-C)\left(u_f\frac{\partial v_f}{\partial x}+v_f\frac{\partial v_f}{\partial z}\right)$$
$$=-\frac{\partial p}{\partial z}+\bar{\mu}\delta^2\left(\delta^2\frac{\partial^2v_f}{\partial x^2}+\beta^2\frac{\partial^2v_f}{\partial y^2}+\frac{\partial^2v_f}{\partial z^2}\right)+C\delta^2\bar{\mu}M(v_p-v_f), \tag{14}$$

$$\frac{\partial}{\partial x}(Cu_p)+\delta\frac{\partial}{\partial z}(Cv_p)=0, \tag{15}$$

$$\bar{\rho}Re\delta(1-C)\bar{\mu}\left(u_p\frac{\partial u_p}{\partial x}+v_p\frac{\partial u_p}{\partial z}\right)$$
$$=-\frac{\partial p}{\partial x}+M(1-C)\bar{\mu}(u_f-u_p), \tag{16}$$

$$\bar{\rho}Re\delta^3(1-C)\bar{\mu}\left(u_p\frac{\partial v_p}{\partial x}+v_p\frac{\partial v_p}{\partial z}\right)$$
$$=-\frac{\partial p}{\partial z}+M(1-C)\bar{\mu}\delta^2(v_f-v_p), \tag{17}$$

under lubrication approach Eqs. (12)-(17) reduced to

$$\frac{\partial p}{\partial x}=\bar{\mu}\left(\beta^2\frac{\partial^2u_f}{\partial y^2}+\frac{\partial^2u_f}{\partial z^2}\right)+MC\bar{\mu}(u_p-u_f), \tag{18}$$

$$\frac{\partial p}{\partial z}=0, \tag{19}$$

$$\frac{\partial p}{\partial x}=M(1-C)\bar{\mu}(u_f-u_p), \tag{20}$$

The corresponding no-slip boundary conditions are

$$u_f=-l_{slip}\frac{\partial u_f}{\partial y}-1 \text{ at } y=1,$$

$$u_f=l_{slip}\frac{\partial u_f}{\partial y}-1 \text{ at } y=-1,$$

$$u_f=-1 \text{ at } z=\pm h(x)=\pm1\pm Kx\pm\phi\sin2\pi x, \tag{21}$$

where $0\leqslant\phi\leqslant1$, $\phi=0$ for straight duct and $\phi=1$ corresponds to total occlusion. Combining Eqs. (18) and (20) we get

$$\beta^2\frac{\partial^2u_f}{\partial y^2}+\frac{\partial^2u_f}{\partial z^2}=\frac{1}{(1-C)\bar{\mu}}\frac{\partial p}{\partial x}. \tag{22}$$

3. Solution of the problem

Using the similar procedure as discussed by Reddy et al. [19] the solution of Eq. (22) satisfying the boundary conditions (21) can be directly written as

$$u_f=-1+\frac{1}{2(1-C)\bar{\mu}}\times\frac{dp}{dx}\left\{z^2-h^2(x)+\frac{4}{h}\sum_{n=1}^{\infty}\frac{(-1)^n\cosh(\alpha_ny/\beta)\cos(\alpha_nz)}{\alpha_n^3(\cosh(\alpha_n/\beta)+l_{slip}\frac{\alpha_n}{\beta}\sinh(\alpha_n/\beta))}\right\}. \tag{23}$$

the particulate velocity will be in the form

$$u_p=-1+\frac{1}{2(1-C)\bar{\mu}}\times\frac{dp}{dx}\left\{\frac{-2}{M}+z^2-h^2(x)+\frac{4}{h}\sum_{n=1}^{\infty}\frac{(-1)^n\cosh(\alpha_ny/\beta)\cos(\alpha_nz)}{\alpha_n^3(\cosh(\alpha_n/\beta)+l_{slip}\frac{\alpha_n}{\beta}\sinh(\alpha_n/\beta))}\right\}. \tag{24}$$

where $\alpha_n=(2n-1)\pi/2h(x)$.

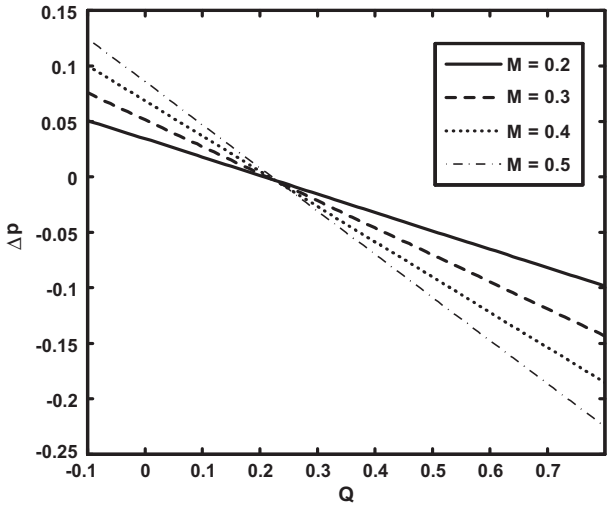

Figure 1 Variation of Δp with Q for different values of M at $\phi=0.6$, $l_{slip}=0.3$, $C=0.5$, $K=0.05$, $\mu=0.7$ and $\beta=1.2$.

The volumetric flow rate in the rectangular duct in the wave frame (in vertical half) is given by

$$q_f = (1-C)\int_0^h \int_0^1 (u_f)dydz,$$
$$= (1-C)\left\{-h + \frac{1}{2(1-C)\bar{\mu}}\frac{dp}{dx} \times \left(-\frac{2}{3}h^3 + 4\frac{\beta}{h}\sum_{n=1}^{\infty}\frac{(-1)^n \sinh(\alpha_n/\beta)}{\alpha_n^5(\cosh(\alpha_n/\beta) + l_{slip}\frac{\alpha_n}{\beta}\sinh(\alpha_n/\beta))}\right)\right\}.$$

$$q_p = C\int_0^h \int_0^1 (u_p)dydz,$$
$$= \frac{C}{(1-C)} \times \left\{\left\{-\frac{h}{M\bar{\mu}}\frac{dp}{dx} + \frac{1}{\bar{\mu}}\frac{dp}{dx} \times \left(-\frac{h^3}{3} + \frac{2\beta}{h}\sum_{n=1}^{\infty}\frac{(-1)^n \sinh(\alpha_n/\beta)}{\alpha_n^5(\cosh(\alpha_n/\beta) + l_{slip}\frac{\alpha_n}{\beta}\sinh(\alpha_n/\beta))}\right)\right\} - h(1-C)\right\}.$$

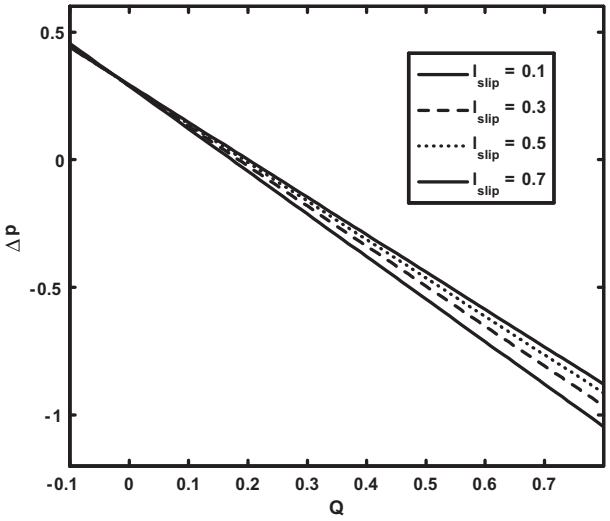

Figure 2 Variation of Δp with Q for different values of l_{slip} at $\phi = 0.5$, $M = 1.3$, $C = 0.3$, $K = 0.005$, $\mu = 0.7$ and $\beta = 1.2$.

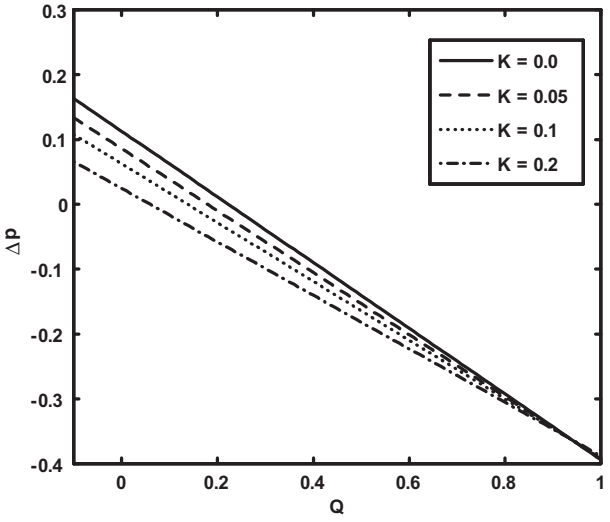

Figure 3 Variation of Δp with Q for different values of K at $\phi = 0.6$, $M = 0.5$, $C = 0.5$, $l_{slip} = 0.3$, $\mu = 0.9$ and $\beta = 1.3$.

where q_f, q_p are the volume flow rate for the fluid phase and particulate phase.

The instantaneous flux in the laboratory frame is

$$Q_f = (1-C)\int_0^h \int_0^1 (u_f + 1)dydz = q_f + h(1-C). \quad (25)$$

$$Q_p = C\int_0^h \int_0^1 (u_p + 1)dydz = q_p + hC. \quad (26)$$

The average volume flow rate over one period $\left(T = \frac{\lambda}{c}\right)$ of the peristaltic wave is defined as

$$\bar{Q}(x,t) = \frac{1}{T}\int_0^T (Q_f + Q_p)dt = q_f + q_p + 1. \quad (27)$$

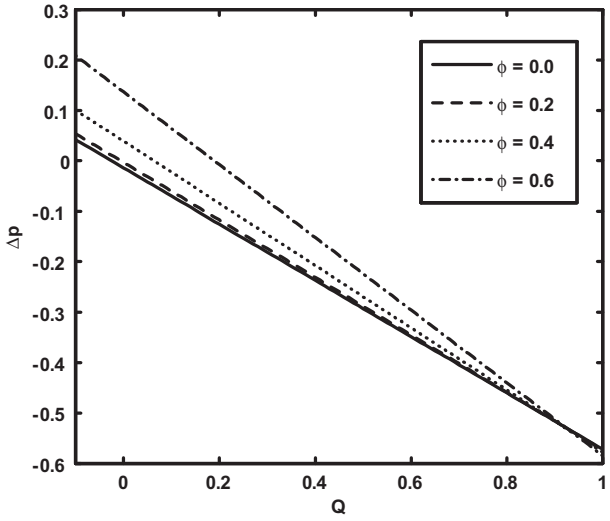

Figure 4 Variation of Δp with Q for different values of ϕ at $K = 0.005$, $M = 0.8$, $C = 0.5$, $l_{slip} = 0.3$, $\mu = 0.9$ and $\beta = 1.3$.

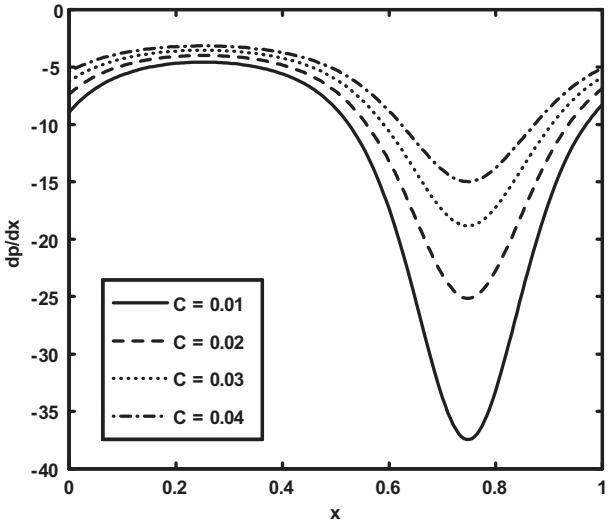

Figure 5 Variation of dp/dx with x for different values of C at $Q = 2.5$, $l_{slip} = 0.3$, $M = 0.2$, $\beta = 1$, $K = 0.005$, $\mu = 0.9$ and $\phi = 0.6$.

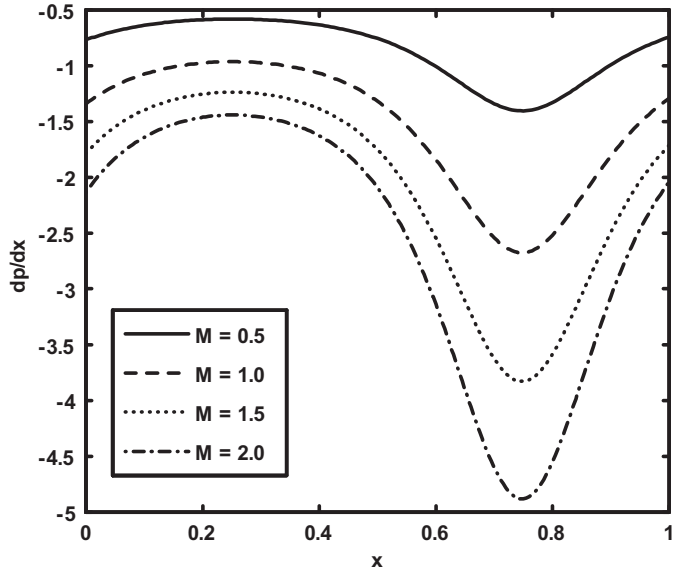

Figure 6 Variation of dp/dx with x for different values of M at $Q = 2.0$, $l_{slip} = 0.4$, $C = 0.5$, $\beta = 1.3$, $K = 0.05$, $\mu = 0.9$ and $\phi = 0.6$.

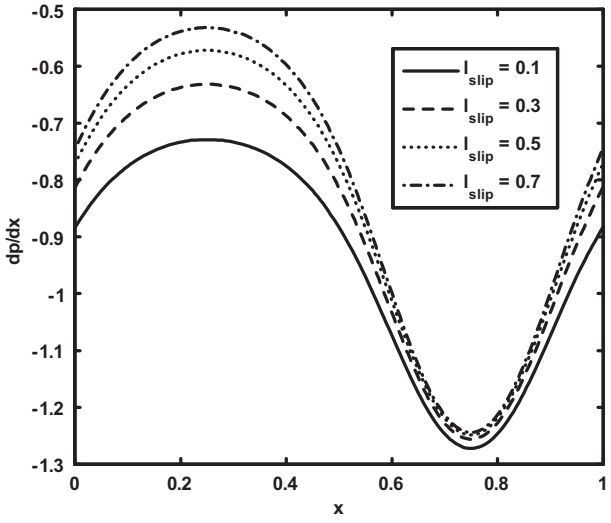

Figure 7 Variation of dp/dx with x for different values of l_{slip} at $Q = 2.0$, $M = 0.4$, $C = 0.5$, $\beta = 1.3$, $K = 0.05$, $\mu = 0.9$ and $\phi = 0.6$.

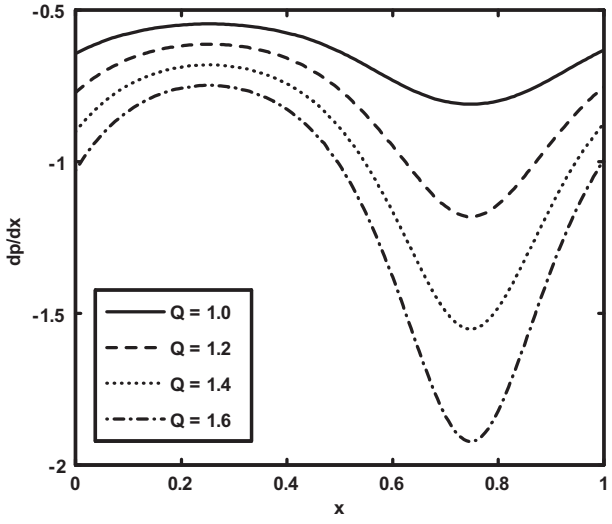

Figure 8 Variation of dp/dx with x for different values of Q at $\beta = 1$, $M = 1$, $C = 0.5$, $\mu = 0.9$, $K = 0.05$, $\phi = 0.6$ and $l_{slip} = 0.6$.

where $\bar{Q}$ the mixture average flux of fluid phase and particulate phase.

From Eqs. (25) and (26) with (29), the pressure gradient is obtained as

$$\frac{dp}{dx} = \frac{3(-1+C)hM(\bar{Q}-1+h)\bar{\mu}}{3Ch^2 + h^4M - 6M\beta\sum_{n=1}^{\infty}\frac{\sinh(\alpha_n/\beta)}{\alpha_n^5(\cosh(\alpha_n/\beta)+l_{slip}\frac{\alpha_n}{\beta}\sinh(\alpha_n/\beta))}}. \quad (28)$$

Integration of Eq. (22) over one wavelength yields

$$\Delta p = \int_0^1 \frac{dp}{dx}dx = \int_0^1 \left\{ \frac{3(-1+C)hM(\bar{Q}-1+h)\bar{\mu}}{3Ch^2 + h^4M - 6M\beta\sum_{n=1}^{\infty}\frac{\sinh(\alpha_n/\beta)}{\alpha_n^5(\cosh(\alpha_n/\beta)+l_{slip}\frac{\alpha_n}{\beta}\sinh(\alpha_n/\beta))}} \right\} dx. \quad (29)$$

It is noticed that when $C \to 0$, $\bar{\mu} \to 0$ and $l_{slip} \to 0$ the solutions of Reddy et al. [19] are recovered as a special case of our problem. Also, in the limit $\beta \to 0$ (keeping a fixed and $d \to \infty$), the rectangular duct reduces to a two dimensional channel and results of Shapiro [1] are recovered.

4. Numerical results and discussion

In this section, the graphical results of the problem under consideration are discussed. The expression for the pressure rise and pressure gradient is calculated using a mathematics software Mathematica.

The variation of pressure rise with volume flow rate Q for different values of M, l_{slip}, K and ϕ is shown in Figs. 1–4. It is observed from Fig. 1 that in the peristaltic pumping

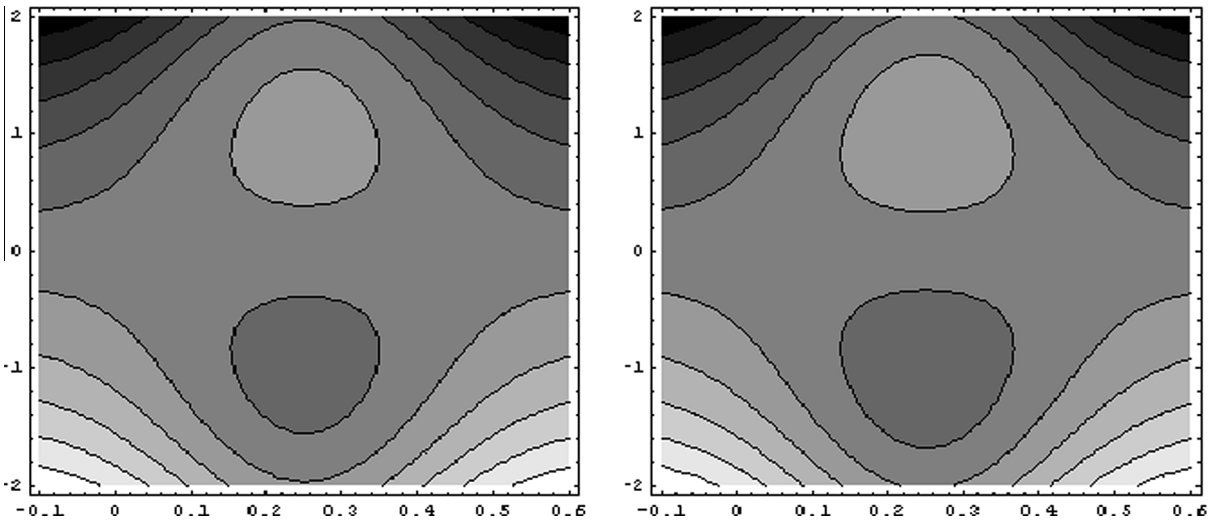

Figure 9 Streamlines for different values of M. (a) for $M = 0.55$ and (b) for $M = 0.6$. The other parameters are $Q = 1$, $\beta = 1.3$, $l_{slip} = 0.3$, $K = 0.04$, $C = 0.5$, $\mu = 0.9$, $y = 0$ and $\phi = 0.4$.

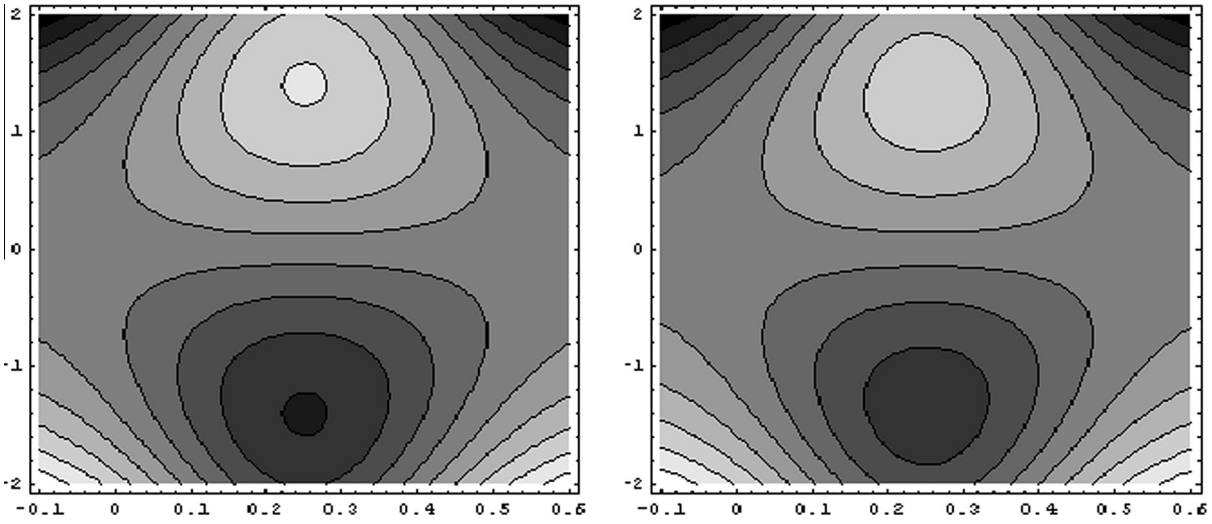

Figure 10 Streamlines for different values of C. (a) for $C = 0.1$ and (b) for $C = 0.15$. The other parameters are $Q = 1$, $\beta = 1.3$, $l_{slip} = 0.3$, $K = 0.04$, $M = 0.5$, $\mu = 0.9$, $y = 0$ and $\phi = 0.6$.

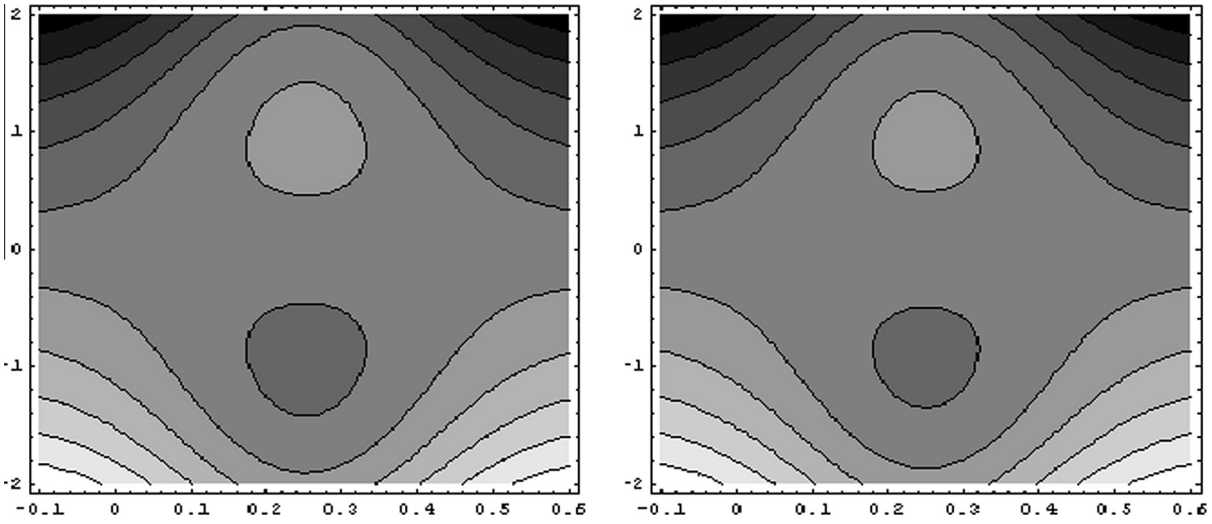

Figure 11 Streamlines for different values of K. (a) for $K = 0.07$ and (b) for $K = 0.01$. The other parameters are $Q = 1$, $\beta = 1.3$, $l_{slip} = 0.3$ $C = 0.5$, $M = 0.5$, $\mu = 0.9$, $y = 0$ and $\phi = 0.6$.

Please cite this article in press as: S. Akram et al., Particulate suspension slip flow induced by peristaltic waves in a rectangular duct: Effect of lateral walls, Alexandria Eng. J. (2016), http://dx.doi.org/10.1016/j.aej.2016.09.011

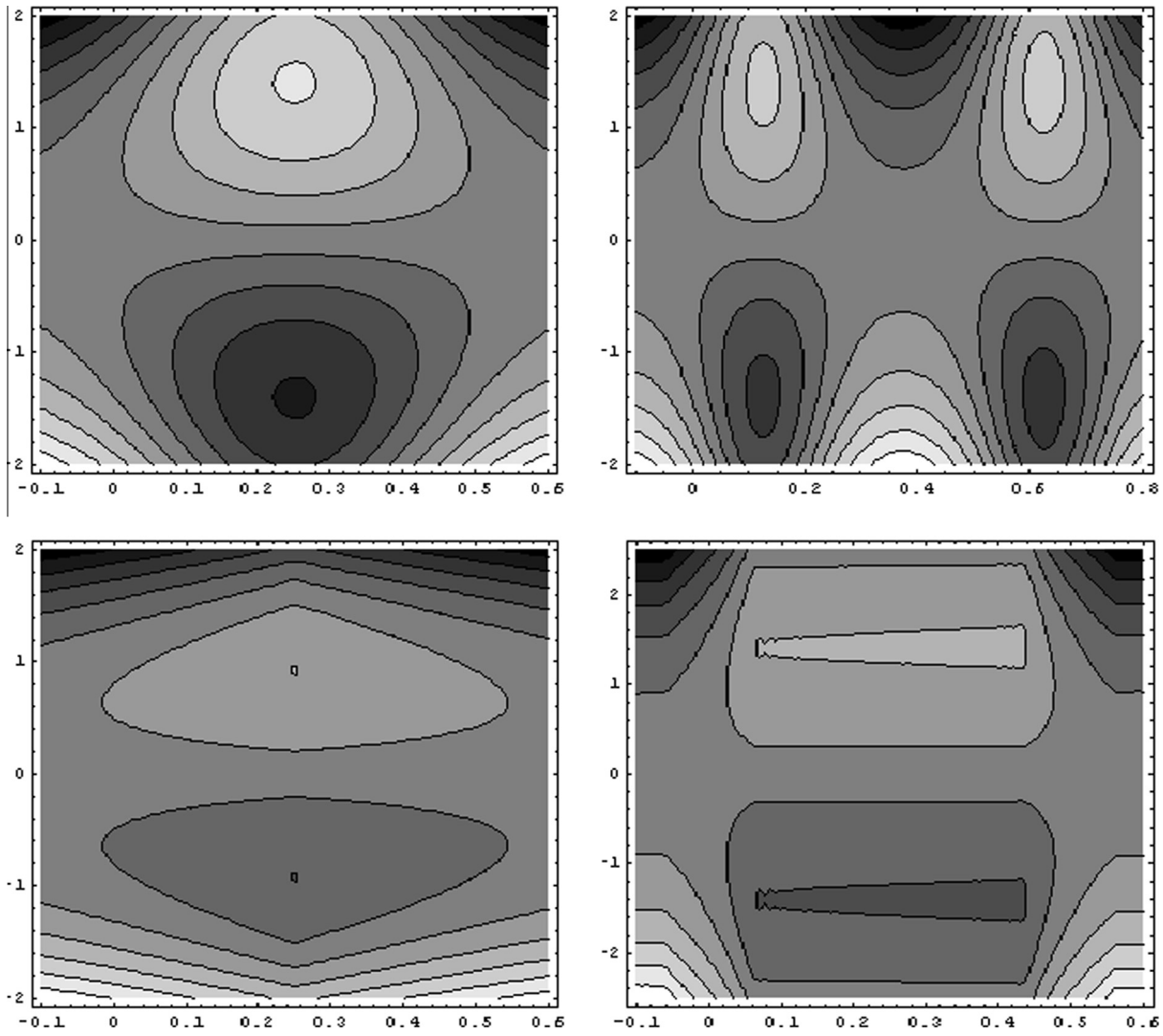

Figure 12 Streamlines for different wave shape The other parameters are $Q = 1$, $\beta = 1.3$, $l_{slip} = 0.3$, $C = 0.1$, $K = 0.04$, $M = 0.5$, $\mu = 0.9$, $y = 0$ and $\phi = 0.6$.

$(\Delta p > 0, Q > 0)$ and retrograde pumping $(\Delta p > 0, Q < 0)$ regions the pumping rate increases with an increase in M, while in the copumping region $(\Delta p < 0, Q > 0)$ the behavior is quite opposite, and here pumping rate decreases with an increase in M. It is depicted from Fig. 2 that in the peristaltic pumping $(\Delta p > 0, Q > 0)$ and retrograde pumping $(\Delta p > 0, Q < 0)$ regions the pressure rise remains constant in these regions, while in the copumping region $(\Delta p < 0, Q > 0)$ the pressure rise decreases with an increase in l_{slip}. Figs. 3 and 4 show the variation of pressure rise with volume flow rate Q. It is observed from Figs. 3 and 4 that the pressure rise decreases in all the regions with an increase in K and pressure rise increases with an increase in ϕ. The pressure gradient for different values of C, M, l_{slip} and Q are plotted in Figs. 5–8. It is depicted from Figs. 5–8 that for $x \in [0, 0.2]$ and $x \in [0.8, 1]$, the pressure gradient is small i.e., the flow can easily pass without imposition of a large pressure gradient, while in the region $x \in [0.2, 0.8]$, the pressure gradient increases with an increase in C, and decreases with an increase in M and Q, so much pressure gradient is required to maintain the flux to pass. It is also observed that the pressure rise increases in the upper half of the channel and decreases in the lower half of the channel with the increase in l_{slip} parameter. Streamlines for different values of M, C and K are shown in Figs. 9–11. It is observed from Fig. 9 that the size of the trapping bolus increases with an increase in M. It is depicted from Fig. 10 that with the increase in C the size and number of the trapped bolus decrease. Fig. 11 shows that the size of the trapped bolus decreases with the decrease in K. Fig. 12 shows the streamlines for different wave form. Figure a is for sinusoidal wave, figure b for multisinusoidal wave, figure c for triangular wave and figure d for trapezoidal wave.

References

[1] M.Y. Jaffrin, A.H. Shapiro, Peristaltic pumping, Annu. Rev. Fluid Mech. 3 (1971) 13–36.
[2] V.P. Srivastava, M.A. Saxena, Two-fluid model of non-Newtonian blood flow induced by peristaltic waves, Rheol. Acta 34 (1995) 406–414.
[3] V.P. Srivastava, Effects of an inserted endoscope on chyme movement in small intestine, Appl. Appl. Math. 2 (2007) 79–91.

[4] V.P. Srivastava, Particle-fluid suspension flow induced by peristaltic waves in a circular cylindrical tube, Bull. Calcutta Math. Soc. 94 (2002) 167–184.
[5] Kh.S. Mekheimer, Y. Abd Elmaboud, Peristaltic flow through a porous medium in an annulus, Appl. An Endosc. 2 (1) (2008) 103.
[6] Kh.S. Mekheimer, Nonlinear peristaltic transport through a porous medium in an inclined planner channel, J. Por. Media 6 (2003) 189–201.
[7] Kh.S. Mekheimer, S.Z.A. Husseny, Y. Abd Elmaboud, Effects of heat transfer and space porosity on peristaltic flow in a vertical asymmetric channel, Numer. Methods Partial Differ. Eqs. (2009), http://dx.doi.org/10.1002/num.20451.
[8] T. Hayat, Y. Wang, A.M. Siddiqui, K. Hutter, Peristaltic motion of a Segalman fluid in a planar channel, Math. Prob. Eng. 1 (2003) 1–23.
[9] L.M. Srivastava, V.P. Srivastava, Peristaltic transport of a particle-fluid suspension, J. Biomech. Eng. 111 (1989) 158.
[10] M.M. Bhattia, M. Ali Abbas, M.M. Rashidi, Combine effects of Magnetohydrodynamics (MHD) and partial slip on peristaltic blood flow of Ree-Eyring fluid with wall properties, Eng. Sci. Technol., Int. J. (2016), http://dx.doi.org/10.1016/j.jestch.2016.05.004.
[11] M.M. Bhatti, A. Zeeshan, N. Ijaz, Slip effects and endoscopy analysis on blood flow of particle-fluid suspension induced by peristaltic wave, J. Mol. Liq. 218 (2016) 240–245.
[12] S. Nadeem, A. Riaz, R. Ellahi, Noreen Sher Akbar, A. Zeeshan, Heat and mass transfer analysis of peristaltic flow of nanofluid in a vertical rectangular duct by using the optimized series solution and genetic algorithm, J. Comput. Theor. Nanosci. 11 (4) (2014) 1133–1149.
[13] A. Riaz, S. Nadeem, R. Ellahi, A. Zeeshan, Exact solution for peristaltic flow of Jeffrey fluid model in a three dimensional rectangular duct having slip at the walls, Appl. Bion. Biomech. 11 (2014) 81–90.
[14] L.M. Srivastava, V.P. Srivastava, Peristaltic transport of a particle-fluid suspension, J. Biomech. Eng. 111 (1989) 157.
[15] J.C. Misra, S.K. Pandey, Peristaltic transport of a particle-fluid suspension in a cylindrical tube, Comput. Math. Appl. 28 (1994) 131.
[16] V.P. Srivastava, L.M. Srivastava, Influence of wall elasticity and poiseuille flow on peristaltic induced flow of a particle-fluid mixture, Int. J. Eng. Sci. 35 (1997) 1359.
[17] V.P. Srivastava, M. Saxena, Particulate suspension flow induced by sinusoidal peristaltic waves, Jpn. J. Appl. Phys. 36 (1997) 385.
[18] Kh.S. Mekheimer, Y. Abd Elmaboud, Peristaltic transport of a particle–fluid suspension through a uniform and non-uniform annulus, Appl. Bion. Biomech. 5 (2) (2008) 47.
[19] M.V. Subba Reddy, M. Mishra, S. Sreenadh, A.R. Rao, Influence of lateral walls on peristaltic flow in a rectangular duct, J. Fluids Eng. 127 (2005) 824.
[20] S. Nadeem, Safia Akram, Peristaltic flow of a Jeffrey fluid in a rectangular duct, Nonlin. Anal.: Real World Appl. 11 (2010) 4238.
[21] S.E. Charm, G.S. Kurland, Blood Flow and Micro-circulation, John Wiley, New York, 1974.

Please cite this article in press as: S. Akram et al., Particulate suspension slip flow induced by peristaltic waves in a rectangular duct: Effect of lateral walls, Alexandria Eng. J. (2016), http://dx.doi.org/10.1016/j.aej.2016.09.011